Na^+ Transport, and the E_1P-E_2P Conformational Transition of the Na^+/K^+-ATPase

Alexandru Babes* and Klaus Fendler†

†Max-Planck-Institut für Biophysik, D-60596 Frankfurt/M, Germany; and *Department of Physiology and Biophysics, Faculty of Biology, University of Bucharest, Bucharest, Romania

ABSTRACT We have used admittance analysis together with the black lipid membrane technique to analyze electrogenic reactions within the Na^+ branch of the reaction cycle of the Na^+/K^+-ATPase. ATP release by flash photolysis of caged ATP induced changes in the admittance of the compound membrane system that are associated with partial reactions of the Na^+/K^+-ATPase. Frequency spectra and the Na^+ dependence of the capacitive signal are consistent with an electrogenic or electroneutral $E_1P \leftrightarrow E_2P$ conformational transition which is rate limiting for a faster electrogenic Na^+ dissociation reaction. We determine the relaxation rate of the rate-limiting reaction and the equilibrium constants for both reactions at pH 6.2–8.5. The relaxation rate has a maximum value at pH 7.4 ($\sim$320 s^{-1}), which drops to acidic ($\sim$190 s^{-1}) and basic ($\sim$110 s^{-1}) pH. The $E_1P \leftrightarrow E_2P$ equilibrium is approximately at a midpoint position at pH 6.2 (equilibrium constant $\approx$ 0.8) but moves more to the E_1P side at basic pH 8.5 (equilibrium constant $\approx$ 0.4). The Na^+ affinity at the extracellular binding site decreases from $\sim$900 mM at pH 6.2 to $\sim$200 mM at pH 8.5. The results suggest that during Na^+ transport the free energy supplied by the hydrolysis of ATP is mainly used for the generation of a low-affinity extracellular Na^+ discharge site. Ionic strength and lyotropic anions both decrease the relaxation rate. However, while ionic strength does not change the position of the conformational equilibrium $E_1P \leftrightarrow E_2P$, lyotropic anions shift it to E_1P.

INTRODUCTION

The Na^+/K^+-ATPase is an ion-translocating membrane protein. It uses the energy derived from the hydrolysis of one molecule of ATP to extrude three sodium ions and import two potassium ions against their electrochemical gradients (Glynn, 1993; Läuger, 1991). Because one positive charge per turnover is transported across the membrane, the Na^+/K^+-ATPase generates outward, hyperpolarizing electrical current; it is "electrogenic." The membrane potential also influences the activity of the Na^+/K^+-ATPase, which is stimulated at depolarized potentials and inhibited by hyperpolarization.

A great deal of research has been directed toward the identification of the electrogenic steps within the reaction cycle of the Na^+/K^+-ATPase (the Albers-Post model). The development of kinetic methods has contributed to a better understanding of how and when electrical charge is moved across the membrane. Whole-cell patch-clamp (Nakao and Gadsby, 1986) and giant excised inside-out patch-clamp (Hilgemann, 1994; Friedrich et al., 1996) techniques have been used to record relaxation currents after voltage jumps that were assigned to a reaction that is rate limited by Na^+ deocclusion at the extracellular side. Current transients after a photolytically generated ATP concentration jump from caged ATP were measured with Na^+/K^+-ATPase-containing membrane fragments adsorbed to a black lipid membrane (BLM) (Fendler et al., 1985, 1987; Borlinghaus et al., 1987; Nagel et al., 1987). This method allowed the assignment of measured rate constants to particular steps of the Na^+ branch of the reaction cycle (Fendler et al., 1987, 1993; Apell et al., 1987). These rate constants can be compared with the results of an optical method using potential sensitive styryl dyes in conjunction with the stopped flow technique to gain kinetic information about the reactions following phosphorylation of the Na^+/K^+-ATPase (Wuddel and Apell, 1995; Kane et al., 1997).

In most cases, time-resolved kinetic measurements of pump currents generated upon flash photolysis of caged ATP were performed using P^3-[1-(2-nitrophenyl) ethyl] caged ATP (NPE-caged ATP), which is released with high efficiency and is commercially available. These measurements are limited to low pH values due to slow photolysis with increasing pH. At pH 7.4 ATP release from NPE-caged ATP has a time constant of $\sim$25 ms, corresponding to a relaxation rate of 40 s^{-1} (McCray et al., 1980; Walker et al., 1988). Recently, a new method has been introduced, which consists of a periodic voltage perturbation of a sequence of reactions involving the phosphorylated sodium pump (Sokolov et al., 1994, 1998; Lu et al., 1995). Although this method uses caged ATP for activation of the enzyme, its time resolution is independent of the rate of release of ATP. Therefore, it allows the measurement of kinetic parameters in a wide pH range. In this paper, we have used the technique to investigate the kinetic parameters of the reactions involved in Na^+ transport at pH 6.2–8.5.

MATERIALS AND METHODS

Chemicals

In most cases the solutions contained 25 mM imidazole, 1 mM dithiothreitol (DTT), 3 mM $MgCl_2$, and 130 mM NaCl. The pH was adjusted to 6.2

Received for publication 26 July 1999 and in final form 26 July 2000.

Address reprint requests to Dr. Klaus Fendler, Max-Planck-Institut für Biophysik, Kennedyallee 70, D-60596 Frankfurt/Main, Germany. Tel.: 49-69-6303-306; Fax: 49-69-6303-305; E-mail: fendler@mpibp-frankfurt.mpg.de.

0006-3495/00/11/2557/15 $2.00

(7.4, respectively) with HCl (referred to as "standard conditions"). For measurements at high pH (8.5), Tris was used instead of imidazole. In sodium-free or low-sodium solutions (Na^+ titration of the capacitive signal), we have used a background of 50 mM imidazole and 0.25 mM EGTA. All chemicals were purchased in analytical grade or higher.

Caged ATP (P^3-[1-(2-nitrophenyl) ethyl] adenosine 5′-triphosphate Na salt) was purchased from Calbiochem. For the lipid bilayers diphytanoylphosphatidylcholine (PC) (synthetic; Avanti Polar Lipids, Pelham, AL) and octadecylamine (60:1, w/v 98%; Riedel-DeHaen AG, Seelze-Hannover, Germany) were prepared 1.5% in *n*-decane according to the method of Bamberg et al. (1979).

Membrane fragments containing Na^+/K^+-ATPase (protein concentration 2–3 mg/ml) from pig kidney were prepared as described previously (Jørgensen, 1974; Fendler et al., 1985). The membrane fragments have diameters of ~100–300 nm (Scales and Inesi, 1976) and a thickness of ~4 nm.

Measuring procedure

Optically black BLMs with an area of 0.01–0.02 cm^2 were formed in a Teflon cell as described elsewhere (Fendler et al., 1987). Each of the two compartments of the cell was filled with 1.5 ml of electrolyte. The membrane was connected to an external measuring circuit via agar-agar salt bridges and Ag/AgCl electrodes. Fifteen microliters of the Na^+/K^+-ATPase-containing membrane fragments (2 mg/ml protein concentration) were added to one compartment of the cuvette and stirred for 40 min, during which the membrane fragments were adsorbed to the BLM in a sandwich-like structure.

The external measuring circuit (Fig. 1 *A*) consists of the lock-in amplifier (model 7220; EG&G Instruments, Wokingham, UK), which applies a sinusoidal alternating voltage across the compound membrane (the BLM together with the adsorbed membrane fragments). The following settings have been used on the lock-in: effective value of the alternating voltage, 10 mV; gain, 0–20 dB; slope, 12 dB/oct; output time constant, 100 ms for frequencies higher than 10 Hz, and 1 s for lower frequencies. The current generated in response to the alternating voltage can either be sent directly to the current input of the lock-in amplifier or passed through a current-voltage converter preamplifier and sent to the voltage input of the lock-in amplifier. The lock-in amplifier then displays the effective values of the two components of the input signal: l_x, in phase with the reference sinusoidal voltage, and l_y, which is 90° out of phase. The advantage of using the preamplifier is that, along with the capacitance measurements, one can also record the short-circuit currents as described by Fendler et al. (1985). The disadvantage is that the preamplifier introduces an additional phase shift and a current amplification, which are both frequency dependent, so that they have to be determined before the experiment.

The adsorption of the membrane fragments was monitored by the decrease in both the l_x and l_y components of the electrical signal on the lock-in amplifier. When the system has reached a steady state (constant values of the two components l_x and l_y), 0.2–0.3 mM caged ATP was added to the compartment containing the membrane fragments and stirred for 10 min. Then, an ATP concentration jump was generated by ATP release through flash photolysis of caged ATP. To photolyze the caged ATP, light pulses of an excimer laser (duration 10 ns, wavelength 308 nm) were focused on the lipid bilayer membrane. The intensity at the membrane surface was adjusted so that 15–20% of the caged ATP was photolyzed.

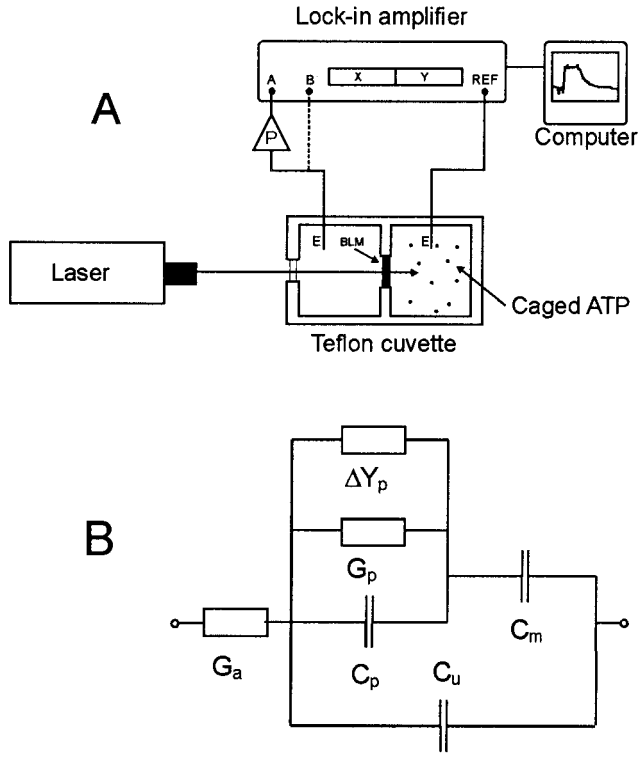

FIGURE 1 (*A*) Bilayer set-up and electrical circuitry used for the measurement of the capacitive signal. A, Voltage input on the lock-in amplifier; B, current input on the lock-in amplifier; REF, output for the alternating voltage; P, preamplifier; BLM, black lipid membrane (with adsorbed membrane fragments containing Na^+/K^+-ATPase); E, Ag/AgCl electrodes. (*B*) Equivalent circuit describing the compound membrane. The capacitance of the membrane fragments, the underlying lipid membrane, and the uncovered lipid membrane are C_p, C_m, and C_u, respectively. The conductivity of the membrane fragments is G_p, and the access conductivity is G_a. The admittance ΔY_p describes the contribution of the Na^+/K^+-ATPase to the electrical properties of the compound membrane.

THEORY

A voltage-sensitive equilibrium under a periodic electrical perturbation

Consider the two-state system

$$A \underset{k^-}{\overset{k^+}{\leftrightarrow}} B \tag{1}$$

Before the perturbation the system is in equilibrium with the concentrations $\overline{c_A^0}$ and $\overline{c_B^0}$. If a periodic perturbation is applied, the system assumes the time-dependent concentrations $c_A(t)$ and $c_B(t)$. We now introduce the time-dependent equilibrium concentrations $\overline{c_A}(t)$ and $\overline{c_B}(t)$. These are the concentrations that would be established if the system were allowed to relax to equilibrium under the conditions prevailing at time t (Bernasconi, 1976). Using these concentrations, we define the reaction variable,

$$x(t) = c_A(t) - \overline{c_A^0} = -c_B(t) + \overline{c_B^0} \tag{2}$$

and the "driving function" (Bernasconi, 1976),

$$\bar{x}(t) = \overline{c_A}(t) - \overline{c_A^0} = -\overline{c_B}(t) + \overline{c_B^0} \tag{3}$$

Using these definitions, we can obtain the "complete relaxation equation" with a method analogous to that of Bernas-

coni (1976) for a second-order system:

$$\frac{dx}{dt} = -\frac{1}{\tau}(x - \bar{x}) \quad \text{with} \frac{1}{\tau} = k^+ + k^- \tag{4}$$

Let us now assume that the reaction described by Eq. 1 is voltage sensitive. The system is perturbed by applying a voltage V over the membrane. The situation can be described by introducing a voltage-dependent equilibrium constant K (Läuger, 1991):

$$K(u) = K^0 e^u \tag{5}$$

K^0 is the equilibrium constant in the absence of a voltage. The dimensionless parameter $u = e_0 V/k_B T$ corresponds to the "real" voltage V expressed in units of $k_B T/e_0 \approx 25$ mV (k_B = Boltzman constant, T = temperature, e_0 = elementary charge). Here we assume that one positive charge is transported over the total transmembrane distance of the membrane when the reaction proceeds from A to B.

Introducing the concentrations for the equilibrium constants, we obtain

$$\frac{\overline{c_B}}{\overline{c_A}} = \frac{\overline{c_B^0}}{\overline{c_A^0}} e^u \tag{6}$$

Under the assumption of a small periodic perturbation ($u \ll 1$) and using $e^u \approx 1 + u$, we obtain

$$\bar{x}(t) = -\frac{\overline{c_A^0} \cdot \overline{c_B^0}}{\overline{c_A^0} + \overline{c_B^0}} u(t) \tag{7}$$

Note that the driving function is 0 if before perturbation the equilibrium is completely on side A or B. It is at maximum for $\overline{c_A^0} = \overline{c_B^0}$.

The equilibrium considered above could be, e.g., a partial reaction of an integral membrane protein in which charge is translocated. The perturbation could be a voltage V applied over the membrane. What is the current response of the system when the perturbation is applied? For this we assume that one positive charge is transported over the total membrane thickness when going from A to B. The current generated per unit area is

$$I = \frac{dq}{dt} = -e_0 \frac{dc_A}{dt} = -e_0 \frac{dx}{dt} \tag{8}$$

Here the concentration c_A is a surface density (molecules per unit area). Using Eq. 8 together with Eq. 4, we obtain

$$I(t) = -e_0 \frac{1}{\tau}(\bar{x} - x) \tag{9}$$

If we use a sinusoidal perturbation and convert to complex numbers, the reaction variable x depends on the driving function $\bar{x}$ according to the method of Bernasconi (1976):

$$x = \frac{1}{1 + i\omega\tau}\bar{x} \tag{10}$$

With Eqs. 7 and 9 we obtain

$$I(t) = \frac{e_0^2}{\tau k_B T} \frac{\overline{c_A^0}\,\overline{c_B^0}}{\overline{c_A^0} + \overline{c_B^0}} \frac{i\omega\tau}{1 + i\omega\tau} V(t) \tag{11}$$

The time-independent complex function relating current and voltage is the admittance Y. It depends on the frequency of the perturbation. The admittance per unit area describing the voltage-sensitive equilibrium A $\leftrightarrow$ B is given by

$$Y_{AB}(\omega) = \frac{e_0^2}{\tau k_B T} \frac{\overline{c_A^0}\,\overline{c_B^0}}{\overline{c_A^0} + \overline{c_B^0}} \frac{i\omega\tau}{1 + i\omega\tau} \tag{12}$$

The real and imaginary parts of $Y_{AB}(\omega)$ are

$$\begin{aligned} \mathrm{Re}\,Y_{AB}(\omega) &= \frac{e_0^2}{\tau k_B T} \frac{\overline{c_A^0}\,\overline{c_B^0}}{\overline{c_A^0} + \overline{c_B^0}} \frac{\omega^2\tau^2}{1 + \omega^2\tau^2} \\ \mathrm{Im}\,Y_{AB}(\omega) &= \frac{e_0^2}{\tau k_B T} \frac{\overline{c_A^0}\,\overline{c_B^0}}{\overline{c_A^0} + \overline{c_B^0}} \frac{\omega\tau}{1 + \omega^2\tau^2} \end{aligned} \tag{13}$$

RESULTS

Using a lock-in amplifier, we have studied the behavior of Na^+/K^+-ATPase reconstituted on BLMs in an alternating electric field. The lock-in amplifier generates a sinusoidal alternating voltage across a compound membrane system consisting of a BLM with adsorbed membrane fragments containing purified Na^+/K^+-ATPase from pig kidney. The lock-in amplifier also monitors the two components of the corresponding alternating current: I_x, in phase with the voltage, and I_y, which is 90° out of phase. All experiments to be discussed further have been performed in the absence of K^+, thus describing the partial reactions of the Na^+/K^+-ATPase associated with Na^+ transport only. If not otherwise indicated, experiments were conducted under "standard conditions" as defined in Materials and Methods.

ATP concentration jumps

We have recorded changes in the values of I_x and I_y associated with activation of Na^+/K^+-ATPase through fast ATP concentration jumps generated by flash photolysis of an inactive precursor, caged ATP. As shown in Fig. 2 *A*, ATP release from caged ATP leads to an increase in both the I_x and the I_y components (ΔI_x and ΔI_y) of the alternating current to a new steady state. The current increment ΔI_y will be used in the following for further analysis. Note that the

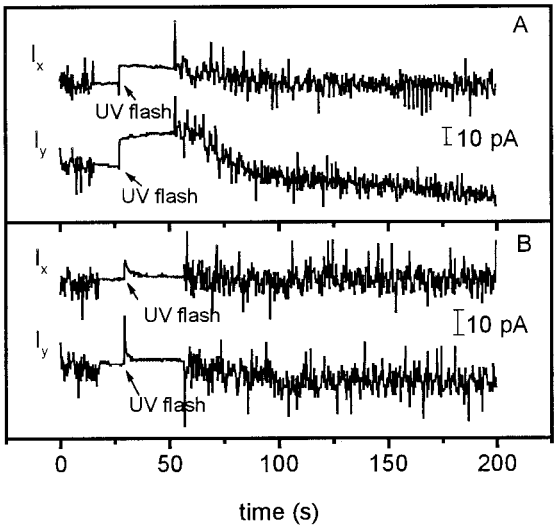

FIGURE 2 (*A*) Fast increase in the I_x and I_y components of the alternating current recorded with the lock-in amplifier upon flash photolysis of caged ATP. Standard conditions, pH 6.2, Na^+/K^+-ATPase 20 μg/ml, caged ATP 0.4 mM. The alternating potential generated by the lock-in was $V = 10$ mV, $\nu = 20$ Hz. Stirring is stopped ~10 s before the laser flash and is resumed ~20 s after the laser flash. The noise associated with stirring is due to mechanically induced capacitance fluctuations of the black lipid membrane. (*B*) Inhibition of the signals I_x and I_y by 150 μM digitoxigenin (same conditions as in *A*).

current increment is rather small: at 20 Hz ΔI_y is only 0.35% of the total component I_y.

When stirring is resumed, we notice a decrease in I_x and I_y toward the initial values (before the flash). This can be explained by the depletion of ATP in the region adjacent to the Na^+/K^+-ATPase-containing membrane fragments due to stirring. The noise associated with stirring is due to capacitance fluctuations of the BLM mechanically induced by stirring. Therefore, for a better signal-to-noise ratio, stirring was stopped during the ATP-releasing laser flash.

Before the flash, in the presence of 130 mM NaCl, the enzyme is stabilized in the E_1 conformation. Upon flash photolysis of caged ATP, the Na^+/K^+-ATPase binds and hydrolyzes ATP and undergoes a conformational transition to the E_2P state. In the absence of K^+, the dephosphorylation is very slow (5 s^{-1}; Hobbs et al., 1988). Therefore, we can assume that upon activation with ATP the phosphorylated Na^+/K^+-ATPase exists in a voltage-dependent equilibrium, $E_1P \leftrightarrow E_2P$. Application of an alternating voltage with amplitude V and a frequency ν (or an angular frequency $\omega = 2\pi\nu$) results in a periodic perturbation of the equilibrium (see Theory), which can be described by an additional admittance. This can be expressed in terms of a capacitance and a conductance increment ΔC_p and ΔG_p in parallel with the conductance G_p and capacitance C_p of the membrane fragments (Eq. A5).

Experimentally, only the total admittance increment ΔY of the compound membrane can be determined, which can be calculated from the in-phase and the out-of-phase components ΔI_x and ΔI_y of the measured current increment. Using complex notation, we obtain $\Delta I_x = V{\cdot}\Delta \mathrm{Re}Y$ and $\Delta I_y = V{\cdot}\Delta \mathrm{lm}Y$, where $\Delta \mathrm{Re}Y$ is the real part and $\Delta \mathrm{lm}Y$ is the imaginary part of ΔY. In a limited frequency range a simple approximate relationship exists between $\Delta \mathrm{lm}Y$ and ΔC_p (Eq. A5), which enables us to calculate ΔC_p from the measured quantity ΔI_y:

$$\Delta C_p = \frac{(C_m + C_p)^2}{C_m^2}\frac{1}{V}\frac{\Delta I_y}{\omega} \tag{14}$$

A similar equation can be derived for ΔG_p, but it yields no additional information. In addition, C_m and C_p are not precisely known. Therefore, only relative values for ΔC_p may be obtained, which makes $\Delta I_y/\omega$ a sufficient and convenient quantity for our analysis.

Inhibition of the capacitive signal by digitoxigenin

Digitoxigenin (a membrane-permeant analog of ouabain) (150 μM) was added under stirring to the compartment containing the Na^+/K^+-ATPase-containing membrane fragments. After 5 min, flash photolysis of caged ATP produced a transient increase in the current (Fig. 2 *B*). After subsequent laser flashes the transient was absent, and only a small stationary increment of the ΔI_y (or ΔI_x) component was observed, which was ~10–20% of the value before the addition of digitoxigenin (Fig. 3). An interesting feature is the presence of a transient signal upon the first laser flash after the addition of the inhibitor (Fig. 2 *B*). This can be explained by the fact that cardiac glycosides bind preferentially to and immobilize the enzyme in the E_2P conforma-

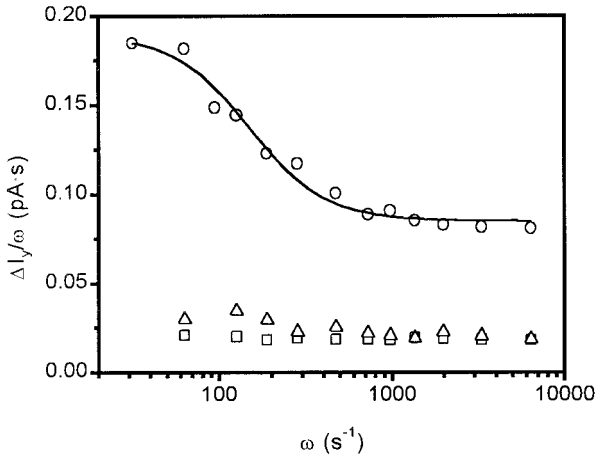

FIGURE 3 Contribution of ATP release from caged ATP to the capacitive signal. Standard conditions, pH 6.2, caged ATP 0.3 mM. Angular frequency spectra were measured in the absence of Na^+/K^+-ATPase (□), upon the addition of 20 μg/ml Na^+/K^+-ATPase (○), and upon further addition of 50 μM digitoxigenin (△). $V = 10$ mV, $\nu = 10$ Hz.

tion of the pump (Glynn, 1985), which requires phosphorylation by ATP.

The experiments demonstrate that the capacitive signal is indeed due to the activity of the Na^+/K^+-ATPase. In particular, the possibility is eliminated that the capacitance increment represents charge separation at the membrane surface due to ATP release from caged ATP. An additional control experiment is shown in Fig. 3. There we have performed flash photolysis experiments in the presence of 0.3 mM caged ATP and no Na^+/K^+-ATPase in the cuvette. Under these conditions we found small increments ΔI_y of 2.5 pA at 20 Hz. The angular frequency spectra of the corresponding capacitance increments ($\Delta I_y/\omega$; see above) showed no angular frequency dependence in the range between 10 and 1015 Hz (below 10 Hz the signal was too noisy to be recorded).

Subsequently, on the same BLM, we have added Na^+/K^+-ATPase-containing membrane fragments to a concentration of 20 μg/ml in one compartment of the cuvette. After 30 min of continuous stirring, flash photolysis of caged ATP induced a much larger change in the ΔI_y component of the alternating current (18 pA at 20 Hz), and the angular frequency spectra of the corresponding capacitance increment displayed a characteristic "Lorentzian" behavior (Fig. 3). Then, 50 μM digitoxgenin was added to the same compartment as the Na^+/K^+-ATPase-containing membrane fragments, and upon stirring for 10 min, the signal due to flash photolysis of caged ATP was decreased to the value before the addition of Na^+/K^+-ATPase. Moreover, the angular frequency spectra were similar to that obtained without Na^+/K^+-ATPase in the cuvette (Fig. 3). Therefore, a fraction of the signal (~12% at low frequencies, up to 22% at 1015 Hz) is probably due to ATP release from caged ATP, but most of the signal, as well as the characteristic "Lorentzian" shape of the angular frequency spectra, reflects the contribution of the Na^+/K^+-ATPase.

Capacitive signal in the presence of monensin and the protonophore 1799

The question was addressed whether the increase in the membrane capacitance can be due to charge accumulation within the space between the attached membrane fragments and the BLM. Upon the addition of 10 μM monensin (a H^+/Na^+,K^+ exchanging agent) and 2.5 μM protonophore 1799 the membrane conductance increased by ~1000 times (from 80 pS to 0.1 μS). Fig. 4 *A* shows the short circuit current recorded as described by Fendler et al. (1985), before and after the addition of ionophores. The trace obtained in the presence of ionophores is characterized by the presence of a small stationary current due to the slow cycling of the pumps in the absence of K^+. In particular, the negative phase observed in the absence of ionophores, which represents backflow of charge from between the membrane fragments and the BLM (Fendler et al., 1985), is

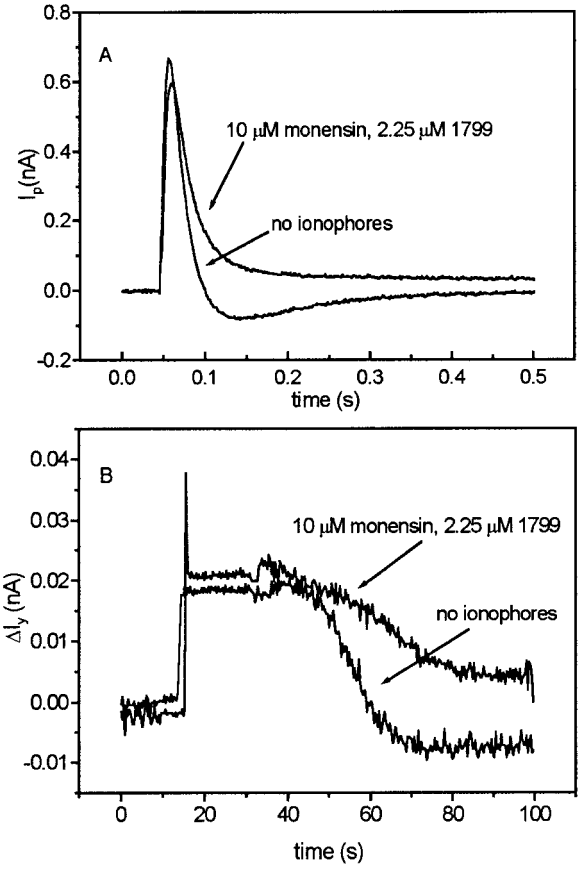

FIGURE 4 (*A*) Transient currents before and after the addition of ionophores. Standard conditions, pH 6.2, Na^+/K^+-ATPase 20 μg/ml, caged ATP 0.225 mM, monensin 10 μM, 1799 2.5 μM. (*B*) Signals recorded on the lock-in amplifier corresponding to the transients presented in *A* (same conditions). The alternating potential generated by the lock-in was characterized by $V = 10$ mV, $\nu = 20$ Hz.

abolished. Fig. 4 *B* shows the corresponding capacitive signals under the same conditions as in Fig. 4 *A*. The difference between the two signals is restricted to the decaying phase when stirring is resumed. In particular, the fast increase and the stationary phase of the I_y component that are associated with changes in the capacitance of the membrane fragments upon flash photolysis of caged ATP are not affected by the presence of the ionophores, which would prevent any charge accumulation after activation of the ion pumps.

Na^+ dependence of the capacitive signal

A NaCl titration of the ΔI_y component of the alternating current was performed, at both low (10 Hz) and high (1015 Hz) frequencies. The result is shown in Fig. 5. The starting solution contained 3 mM $MgCl_2$, 50 mM imidazole, 0.25 mM EGTA, and 1 mM DTT at pH 6.2. Although half-saturation of the titration curves occurs at ~90 mM, a simultaneous fit according to the model described in the Discussion gave a binding constant of 900 mM. The low

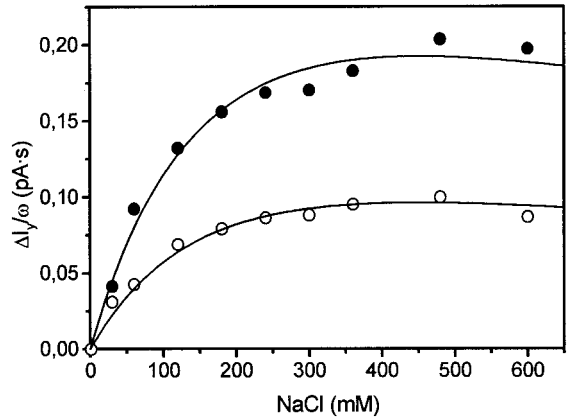

FIGURE 5 Na^+ dependence of the capacitive signal at 10 Hz (●) and 1015 Hz. (○). Initial conditions: $MgCl_2$ 3 mM, DTT 1 mM, imidazole 50 mM, EGTA 0.25 mM, Na^+/K^+-ATPase 20 μg/ml, caged ATP 0.3 mM, pH 6.2, $V = 10$ mV. For fitting procedure see Discussion.

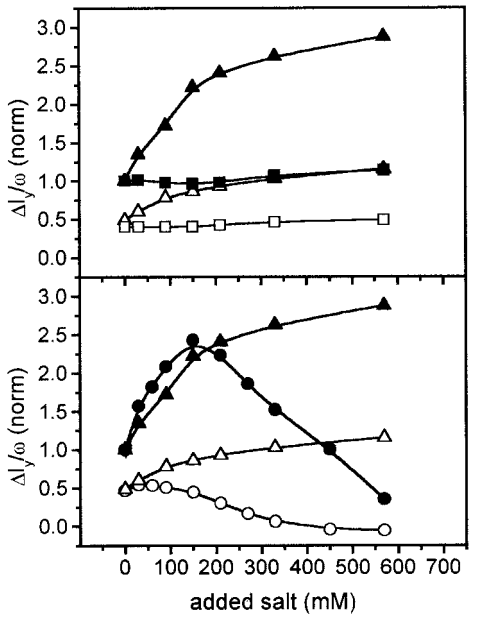

FIGURE 6 The capacitive signal at 10 Hz (●, ■, ▲) and 1015 Hz. (○, □, △) at different concentrations of added salts. Initial conditions: $MgCl_2$ 3 mM, NaCl 50 mM, DTT 1 mM, imidazole 50 mM, Na^+/K^+-ATPase 20 μg/ml, caged ATP 0.3 mM, pH 6.2, $V = 10$ mV. (*Top*) Addition of choline chloride (□, ■). (*Bottom*) Addition of $NaClO_4$ (○, ●). For comparison a reference measurement generated by the addition of NaCl has been included in both graphs (△, ▲). The results are normalized to the value obtained at 10 Hz before the addition of salt.

affinity suggests that the Na^+ dependence of the ΔI_y component of the measured current describes the effect of sodium ions on the $E_1P \leftrightarrow E_2P$ equilibrium at the extracellular binding sites.

To exclude the influence of ionic strength on the capacitive signal, the ΔI_y component of the current was measured at 10 and 1015 Hz, using a buffer that contained 50 mM NaCl and increasing amounts of choline chloride (other buffer components were as described above for the Na^+ titration). As a reference, a NaCl dependence has been obtained as described above, but starting at 50 mM NaCl. The two dependencies are shown in Fig. 6 (*top*). They have been normalized to the low frequency value (10 Hz) at 50 mM NaCl. The comparison demonstrates that ionic strength does not affect the high and low frequency capacitive signal at total salt concentrations ([NaCl] + [choline chloride]) up to 630 mM. It also rules out a lyotropic effect of the Cl^- anions in this concentration range.

Lyotropic anions modulate the properties of the Na^+/K^+-ATPase (Suzuki and Post, 1997; Ganea et al., 1999). The effect of the lyotropic anion ClO_4^- is shown in Fig. 6 (*bottom*). This is a titration similar to that described above starting at 50 mM NaCl. But in this case $NaClO_4$ was added. These data were normalized to the reference NaCl dependence used in Fig. 6 (*top*) as described. A pronounced effect of the replacement of Cl^- by ClO_4^- is found and can be explained by a shift of the conformational equilibrium to the E_1P form induced by the lyotropic anion as described before (Suzuki and Post, 1997).

ATP dependence of the capacitive signal

The ATP dependence of the capacitive signal has been determined in two different ways, using a titration protocol described previously for transient currents generated by the Na^+/K^+-ATPase (Nagel et al., 1987). First, a caged ATP titration of the signal was performed by successive caged ATP additions. The ATP concentration upon flash photolysis of caged ATP was calculated from the light intensity at each caged ATP concentration as described elsewhere (Friedrich et al., 1996). The signal displayed a saturating behavior, with a $K_{0.5}$ of 0.35 μM ATP. Subsequently, the concentration of released ATP was decreased by decreasing the released fraction at a constant saturating caged ATP concentration of 400 μM via a reduction of the light intensity. Under these conditions the ATP dependence had a $K_{0.5}$ of 24 μM. This behavior is typical for competitive binding of caged ATP to the ATP binding site (Nagel et al., 1987).

Frequency spectra of the capacitive signal

We have recorded capacitive signals at frequencies of the applied sinusoidal voltage between 3 and 1015 Hz. The limits of this frequency domain have been chosen to maintain a direct proportionality between the small changes in the capacitance of the adsorbed membrane fragments and the corresponding small changes in the ΔI_y component of the current (see Discussion). The lower frequency is limited by the time constant of the compound membrane, while the upper limit is determined by the access resistance through the agar bridges and the electrolyte solution. Lowering the

access resistance allows the extension of the frequency domain toward higher values. Under the conditions of the experiment the low and the high frequency limits were ~3 Hz and ~1000 Hz, respectively.

In Fig. 7 the capacitive signal is plotted as a function of the angular frequency ω at three different pH values. Under these conditions, the frequency dependence of the capacitive signal reflects the voltage-dependent equilibrium $E_1P \leftrightarrow E_2P$. It can be shown (Eqs. 13 and 14) that the measured quantity ΔC_p is proportional to a Lorentzian function $1/(1 + \omega^2\tau^2)$, where τ represents the relaxation time of the equilibrium. It is obvious from Fig. 7 that this is not sufficient to describe the data, and an additional constant term has to be added. Therefore, for a fit of the experimental results, the following model function was used:

$$\Delta C_p = A + \frac{B}{1 + \omega^2\tau^2} \quad (15)$$

As shown in Fig. 7, at pH 7.4 the maximum value for the relaxation rate was obtained, $\tau^{-1} = 323\ s^{-1}$. At pH 8.5, τ^{-1} decreased to 114 s^{-1}, and at pH 6.2 it decreased to 192 s^{-1}. These values are compiled in Table 1. Note that the data for pH 7.4 shown in the figure are the same as those of Ganea et al. (1999). There, a somewhat larger value of $\tau^{-1} = 393 \pm 51\ s^{-1}$ was obtained because of a different fitting procedure.

TABLE 1 Kinetic parameters for the $E_1P \leftrightarrow E_2P$ transition and for extracellular Na^+ binding at three different pH values

	pH 6.2	pH 7.4	pH 8.5
$\Delta C_p^{1015}/\Delta C_p^{10}$	**0.45**	**0.36**	**0.30**
K_{12}	**0.82**	**0.56**	**0.43**
τ^{-1} (s^{-1})	**192**	**323**	**114**
k^+ (s^{-1})	**166**	225	59
$\tilde{k}^-$ (s^{-1})	**26**	98	55
k^- (s^{-1})	**203**	401	138
K_{Na} (mM)	**900**	400	200

Bold face: calculated from the data shown in Figs. 5 and 7. Normal face: calculated on the basis of $K_{Na} = 400$ mM and $K_{Na} = 200$ mM.

The amplitudes of the capacitive signal at different pH

The high and the low frequency limits of the capacitive signal (in the following these will be referred to as amplitudes) were measured at several pH values. The pH was varied by successive additions of HCl or NaOH, starting at different pH values (Fig. 8). The measurements were carried out at two different frequencies, 10 Hz and 1015 Hz. The amplitude values were normalized to the maximum value at 10 Hz for each experiment. The low frequency amplitude (10 Hz) displays a more pronounced pH dependence, with a maximum amplitude close to pH 8. The amplitude of the high-frequency component (1015 Hz) is almost constant between pH 6 and 8 and starts to decline at higher pH values.

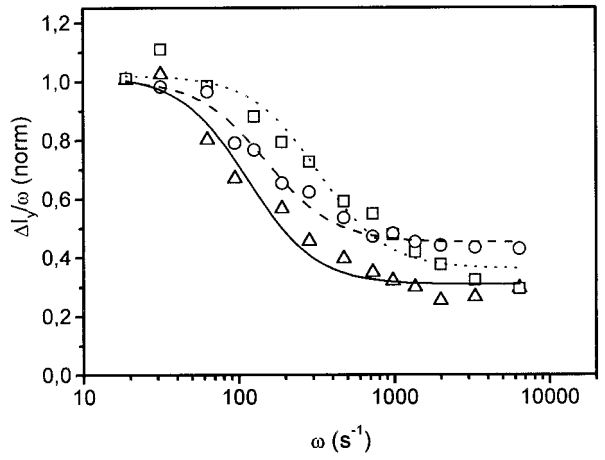

FIGURE 7 Frequency spectra of the capacitive signal at pH 6.2 (○), pH 7.4 (□), pH 8.5 (△). Conditions: NaCl 130 mM, $MgCl_2$ 3 mM, DTT 1 mM, imidazole 25 mM (or Tris 25 mM, for pH 8.5), Na^+/K^+-ATPase 20 μg/ml, caged ATP 0.225 mM. The spectra were fitted with $\Delta I_y/\omega = A + B/(1 + \omega^2\tau^2)$. The relaxation rates τ^{-1} obtained were 192 s^{-1} (pH 6.2), 323 s^{-1} (pH 7.4), and 114 s^{-1} (pH 8.5).

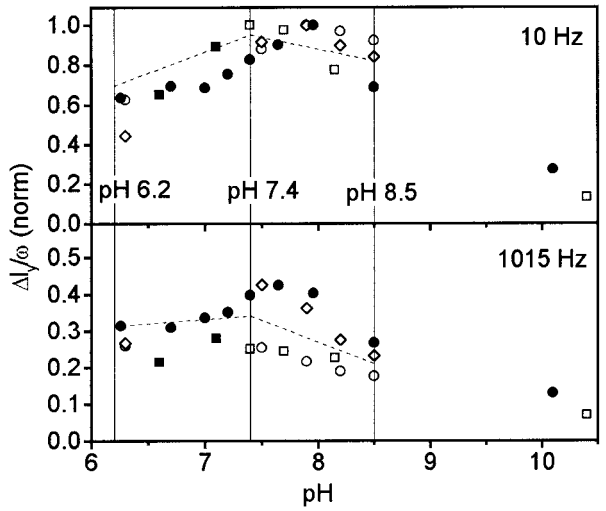

FIGURE 8 pH dependence of the capacitive signal ($\Delta I_y/\omega$) at 10 Hz and 1015 Hz. Five different experiments were performed: 1) Starting solution: imidazole 25 mM, pH 7.4. The pH was decreased by the addition of HCl (■). 2) Using the same starting solution as in (1), the pH was increased by the addition of NaOH (□). 3) and 4) Starting solution: Tris 25 mM, pH 8.5. The pH was decreased by the addition of HCl (○ and ◇). 5) Starting solution: imidazole 25 mM, pH 6.2. The pH was increased by the addition of NaOH (●). In all experiments the electrolyte solutions contained NaCl 130 mM, $MgCl_2$ 3 mM, DTT 1 mM, Na^+/K^+-ATPase 20 μg/ml, and caged ATP 0.3 mM. The amplitude values were normalized to the maximum value at 10 Hz for each experiment.

DISCUSSION

In which frequency range is the approximation valid?

The ion pumps are electrically characterized by an increment of the complex admittance, $\Delta Y_p(\omega) = \Delta G_p + i\omega\Delta C_p$, of the membrane fragments. $\Delta Y_p(\omega)$ is part of a complicated RC network describing the electrical properties of the compound membrane (see Fig. 1 *B*), which consists of the supporting bilayer and the adsorbed membrane fragments (Bamberg et al., 1979). The compound membrane has the total admittance $Y(\omega)$. Using the lock-in amplifier, we determine changes in the total admittance, $\Delta Y(\omega) = \Delta \mathrm{Re}Y + i\Delta \mathrm{lm}Y$, upon activation of the ion pumps. To calculate $\Delta Y_p(\omega)$ from $\Delta Y(\omega)$, we exploit the fact that these two quantities are approximately proportional (see Eq. A5 in the Appendix). This relationship is only valid in a limited frequency range that will be determined in the following.

To test the response of the equivalent circuit at the different frequencies, we calculated the total admittance of the equivalent circuit before ($\Delta Y_p = 0$) and after activation of the Na^+/K^+-ATPase by photolytic release of ATP ($\Delta Y_p(\omega) = \Delta G_p + i\omega\Delta C_p$), as described in the Appendix. A constant, frequency-independent value was assumed for the real (ΔG_p) and for the imaginary ($\omega\Delta C_p$) parts of ΔY_p (corresponding to the situation at the characteristic frequency $\omega = 1/\tau$; see Eq. 13). The difference in total admittance before and after activation yields the increment $\Delta Y(\omega)$. From $\Delta \mathrm{Re}Y$ and $\Delta \mathrm{Im}Y$ the real and the imaginary components of $Y_p(\omega)$ can be calculated according to the approximation A5 and can be compared to the exact values as shown in Fig. 9.

The horizontal solid line in Fig. 9 at 1.5 pAV^{-1} corresponds to the exact value of ΔG_p and $\omega\Delta C_p$ as chosen for the calculation. The dashed lines show the result of the approximation (Eq. A5). It is clear that the approximation is valid only for a certain frequency range. If we define the lower and the upper bound of the range as the angular frequency at which the approximate value is 50% of the exact value, we obtain from Fig. 9 $2\ s^{-1} \ll \omega \ll 2500\ s^{-1}$ for $\omega\Delta C_p$ and for $10\ s^{-1} \ll \omega \ll 10000\ s^{-1}$ ΔG_p.

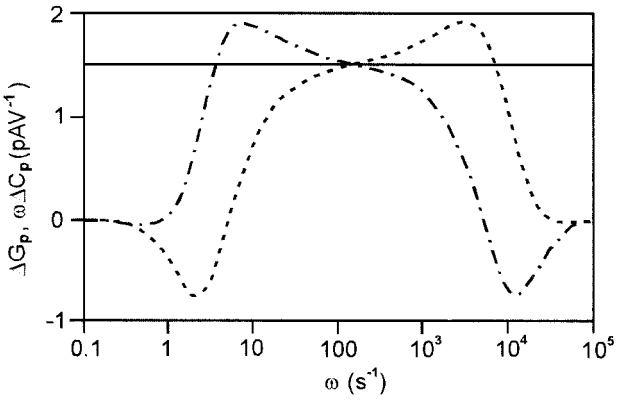

FIGURE 9 Comparison of the exact solution with the approximation given in Eq. 16. ——, ΔG_p; – · – · –, ΔC_p. The horizontal solid line corresponds to the exact solution.

The low frequency limit is reached when the condition $\omega C_p \gg G_p$, as used in the approximation, no longer holds. With a typical capacitance of the membrane fragments of $\sim 1\ \mu F/cm^2$ and a conductance of $\sim 3\ \mu S/cm^2$, the ratio G_p/C_p is $\sim 3\ s^{-1}$. This agrees well with Fig. 9. Another limit exists at high frequencies because in the approximation the access resistance $1/G_a$ was neglected. This resistance is composed of the resistance of the solution and the salt bridges and the input resistance of the lock-in amplifier and has a value of $\sim 40\ k\Omega$. Together with the capacitance of the compound membrane, this represents a low-pass RC network that limits the range of the measurement to angular frequency values below G_a/C_{tot}. The total capacitance of the compound membrane C_{tot} has a typical value of ~ 2 nF, yielding an upper limit of $\omega \ll 1.25 \times 10^4\ s^{-1}$. This crude estimation is somewhat higher than the value obtained by the calculation of $\omega\Delta C_p$ shown in Fig. 9, which is $\omega \ll 2.5 \times 10^3\ s^{-1}$ (but agrees with the upper limit for ΔG_p).

The analysis shown in Fig. 9 demonstrates that the real component or the imaginary component of ΔY can be used to characterize the ion pumps contained in the membrane fragments. We have chosen to use $\Delta \mathrm{Im}Y$, which gives a range of $2\ s^{-1} \ll \omega \ll 2500\ s^{-1}$ in which Eqs. A5 and 14 apply and in which $\Delta C_p(\omega)$ can be calculated. This "angular frequency window" also gives us the range of relaxation times that can be determined. The range given above shows that the method is well suited for relaxation times of 100–400 s^{-1} as determined here.

The capacitive signal reflects an electrogenic reaction of the Na^+/K^+-ATPase

Digitoxigenin is a membrane-permeant analog of ouabain, a specific inhibitor of the Na^+/K^+-ATPase. Upon the addition of 150 μM digitoxigenin to the same compartment as the Na^+/K^+-ATPase, a drastic reduction in the lock-in signal, on both I_x and I_y components and at both low (10 Hz) and high (1015 Hz) frequencies, was observed. The remaining signal is comparable to the signal in the absence of Na^+/K^+-ATPase and is probably due to the polarization of the membrane-liquid interface after the release of ATP from caged ATP. It shows no frequency dependence between 10 and 1015 Hz (Fig. 3) and will be neglected in the following. In addition, the measurements carried out in the presence of ionophores (Fig. 4) demonstrate that the signal must be attributed to charge movements associated with partial reactions of the Na^+/K^+-ATPase, and not to charge accumulation as a result of overall pumping activity. We can, therefore, assign the capacitive signal to a charge-translocating reaction in the reaction cycle of the Na^+/K^+-ATPase. In the following, we will discuss the assignment of

this process to a well-defined partial reaction of the ion pump.

The capacitive signal contains contributions from a slow and a fast reaction

From a single electrogenic reaction a Lorentzian frequency dependence of the capacitive signal is expected (see Eq. 13) that decays to zero at high frequencies. However, as shown in Fig. 7, at high frequencies the capacitive signal attains a constant amplitude of ~30% of the value at low frequency. This component is clearly a result of the enzymatic activity of the Na^+/K^+-ATPase (Fig. 3). A similar behavior has been observed previously (Lu et al., 1995; Sokolov et al., 1998). It has been interpreted in terms of an electrogenic reaction with a relaxation rate outside the experimental frequency spectrum, possibly the movement of Na^+ ions inside a putative access channel (Lu et al., 1995).

From the frequency dependence (Fig. 7) we have to conclude that two reactions contribute to the capacitive signal: 1) a slow reaction, which at pH 7.4 has a relaxation rate of $\tau^{-1} = 323\ s^{-1}$ (Fig. 7); 2) a fast reaction, for which only a lower limit for the relaxation rate of $\tau^{-1} > 7000\ s^{-1}$ can be given. In the following we analyze the amplitude of the capacitive signal at high frequency (1015 Hz), ΔC_p^{1015}, and at low frequency (10 Hz), ΔC_p^{10}, at different Na^+ concentrations and pH. It is shown that the behavior of the amplitudes is compatible with the assumption that the slow step is the $E_1P \leftrightarrow E_2P$ transition, while the fast reaction is extracellular Na^+ binding/release.

The capacitive signal and the reaction cycle of the Na^+/K^+-ATPase

Before the laser flash, in the presence of 130 mM NaCl, the Na^+/K^+-ATPase is in the NaE_1 state, according to the Albers-Post model. Upon flash photolysis of caged ATP and ATP release, the pumps bind and hydrolyze ATP, become phosphorylated, and occlude Na^+, forming $(Na)E_1P$. Then they undergo a conformational transition to the E_2PNa state (for simplicity called the $E_1P \leftrightarrow E_2P$ transition) and finally release Na^+. The reaction sequence can be described in a simplified model: $NaE_1 + ATP \rightleftharpoons NaE_1ATP \rightleftharpoons (Na)E_1P \rightleftharpoons E_2PNa \rightleftharpoons E_2P + Na^+$. The three transported Na^+ ions have been proposed to be sequentially released at the extracellular side (Stürmer et al., 1991; Hilgemann, 1994). However, these reactions are probably very fast (>250,000 s^{-1}, Hilgemann, 1994; >300,000 s^{-1}, Lu et al., 1995, at 37°C). For the purposes of our experimental technique, which is of limited time resolution (<2500 s^{-1}; see above), these steps may be lumped together into a single Na^+ dissociation reaction.

In the absence of K^+ the dephosphorylation is slow (<7 s^{-1} at pH 6–9; Forbush and Klodos, 1991) compared to the formation of the phosphoenzyme (>100 s^{-1} at pH 6.2–8.5; Kane et al., 1997). Therefore, we may assume that immediately after the flash most of the pumps are in a phosphorylated state and remain there for many seconds until the released ATP in the vicinity of the membrane starts to decrease. The increase in the components of the observed current upon flash photolysis of caged ATP reflects the existence of a voltage-dependent equilibrium between the phosphorylated intermediates as proposed previously, based on whole-cell patch-clamp measurements on cardiac myocytes (Nakao and Gadsby, 1986; Lu et al., 1995) and electrical measurements on membrane fragments from rabbit kidney (Sokolov et al., 1998).

When the capacitive signal was recorded at increasing concentrations of caged ATP, its amplitude displayed a saturating behavior with a $K_{0.5}$ of 0.35 μM ATP. In contrast, pre-steady-state kinetic measurements have yielded a binding constant for ATP of ~10 μM from the ATP dependence of the relaxation rate (Fendler et al., 1987; Kane et al., 1997). How can this discrepancy be explained? Our present method is a steady-state relaxation technique, and the amount of phosphorylated protein formed is controlled not only by the concentration of ATP, but also by the rate of recovery of the E_1 state upon dephosphorylation. As a consequence of slow dephosphorylation in the absence of K^+, very low ATP concentrations are sufficient to saturate the capacitive signal, which yields a higher apparent affinity for ATP.

The kinetic model

In the following we analyze the Na^+ dependence of the amplitudes of the capacitive signal on the basis of a simplified kinetic model that comprises the $E_1P \leftrightarrow E_2P$ conformational transition and a Na^+ binding/release step as shown in Fig. 10. Here it is assumed that all Na^+ binding

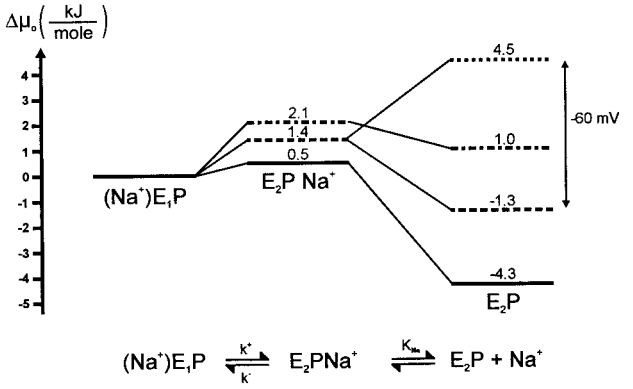

FIGURE 10 Relative basic free energy levels for states of the Na^+/K^+-ATPase involved in sodium translocation at pH 6.2, 7.5, and 8.5 (*bottom to top*), calculated according to the kinetic parameters from Table 1. Free energies of the levels are given in kJ/mol. (*Bottom*) Kinetic model for Na^+ translocation.

sites must be occupied before E_1P can be formed, and Na^+ represents all three transported Na^+ ions.

The question of which of the steps of the Na^+ transport reaction are electrogenic has been the subject of discussion (Rakowski et al., 1997). Complications in the assignment of the electrogenic steps arise from the fact that if a very rapid Na^+ binding/release step is assumed ($\tau_{Na} \rightarrow 0$), the model shown in Fig. 10 is kinetically equivalent to the simple one-step model, $(Na)E_1P \leftrightarrow X_{Na}$. The forward rate constant is k^+, and the backward rate constant is Na^+ concentration (c_{Na}) dependent, $\tilde{k}^- = k^- c_{Na}/(c_{Na} + K_{Na})$. X_{Na} comprises the E_2PNa and E_2P intermediates. This simple model shows how with increasing Na^+ concentration the equilibrium is shifted in favor of $(Na)E_1P$. Under conditions in which the experimental time resolution is not sufficient to resolve a rapid Na^+ binding/release step, the assumption $\tau_{Na} \rightarrow 0$ holds. Consequently, the kinetic system behaves according to a one-step electrogenic reaction without the possibility of assessing whether the $E_1P \leftrightarrow E_2P$ conformational transition or the Na^+ binding/release step or both are electrogenic. Therefore, electrogenicity of a single partial reaction cannot be inferred from a relaxation experiment alone. However, the Na^+ dependence of the effect can contribute additional information. This approach has been used in the past (Gadsby et al., 1993) and will also be applied to the capacitive measurements presented here.

It became clear very early from voltage jump measurements on cardiac myocytes that only the reverse reaction of the electrogenic reaction is voltage sensitive (Gadsby et al., 1992). This would be a straightforward result of the kinetic model (Fig. 10) if it is assumed that only the Na^+ binding reaction is electrogenic. Also, the voltage dependence of Na^+/Na^+ exchange on squid axon could be explained using an electrogenic Na^+ binding reaction, rate limited by an electroneutral $E_1P \leftrightarrow E_2P$ transition (Gadsby et al., 1993). In addition, using fast current recording equipment, current transients were observed on cardiac myocytes, membrane fragments from rabbit kidney, and squid giant axons, which were assigned to a fast Na^+ dissociation reaction (Hilgemann, 1994; Wuddel and Apell, 1995; Rakowski et al., 1997). This has been supported by capacitance measurements on cardiac myocytes (Lu et al., 1995). On the other hand, there seems to be indirect evidence from experiments using lyotropic anions for an electrogenic $E_1P \leftrightarrow E_2P$ transition (Ganea et al., 1999). However, the results of the latter study do not rule out the possibility that the contribution of the $E_1P \leftrightarrow E_2P$ transition to the overall charge translocation across the entire membrane might be small, as proposed by various studies (Wuddel and Apell, 1995; Gadsby et al., 1993). The results of Ganea et al. (1999) could perhaps be explained by a large local electric field effect of lyotropic anions on a small charge translocation during the $E_1P \leftrightarrow E_2P$ transition.

The selection of an appropriate model is crucial, because conclusions from a kinetic analysis are, in general, model dependent. In the following, we will analyze the capacitive signals on the basis of the kinetic model shown in Fig. 10, with emphasis on the Na^+ dependence of the amplitudes. The relaxation of the Na^+ binding reaction is assumed to be much faster than the applied periodic perturbation ($\omega \ll (\tau_{Na})^{-1}$). The data presented here and those by other groups (Lu et al., 1995; Sokolov et al., 1998) clearly rule out the $E_1P \leftrightarrow E_2P$ transition as the exclusive electrogenic step. In addition, its contribution to the overall electrogenicity of Na^+ transport is probably small, as discussed above. We have therefore chosen to use a kinetic model with an electroneutral conformational transition. This model is a convenient basis for our kinetic analysis for the following reasons. The data presented in this study are consistent with such a model (but also with one that attributes part of the electrogenicity to the conformational transition). An electrogenic $E_1P \leftrightarrow E_2P$ transition would require an additional parameter, namely the relative electrogenicity of the conformational transition, which cannot be determined on the basis of our experimental data. An electroneutral conformational transition keeps the mathematics simple. For completeness, we discuss below in a qualitative way the effect of additional electrogenicity in the conformational transition.

The amplitudes of the capacitive signal

The interpretation of the Na^+ dependence of the amplitudes is complex because different effects contribute. On the one hand, it is the amount of phosphoenzyme that controls the amplitudes of the capacitive signal. On the other hand, the ratio of the E_1P and the E_2P concentrations also determines the magnitude of the signal. The latter is apparent from the frequency-independent term in Eq. 13. Therefore, we have to take into account the following processes: 1) In the low concentration range, more and more E_1P and E_2P intermediate is formed with increasing Na^+ concentration as it binds to its cytoplasmic binding site, thereby allowing phosphorylation. 2) In the high concentration range, binding of Na^+ to the extracellular binding sites speeds up the back-reaction of the $E_1P \leftrightarrow E_2P$ equilibrium and drives the enzyme into the E_1P state. 3) High Na^+ concentrations require high anion concentrations (Cl^- in our case), which increase E_1P via a lyotropic effect (Suzuki and Post, 1997; Ganea et al., 1999). 4) At high concentrations Na^+ can replace K^+ in dephosphorylating the enzyme (Nagel et al., 1987). Via rephosphorylation this effect also increases the E_1P concentration.

Formation of the phosphoenzyme (process 1) takes place at low concentrations of Na^+. The half-saturation concentration of this process is reached at a Na^+ concentration at which the rate of formation and decay of the phosphoenzyme have the same magnitude. Because the decay of E_2P is very slow (5 s^{-1}, Hobbs et al., 1988; <7 s^{-1}, Forbush and Klodos, 1991), this concentration is very low. From the Na^+ dependence of the transient electrical signal (Nagel et al.,

1987) we estimate it to be ~1 mM. The increase in the amplitudes with rising Na^+ concentration shown in Fig. 5 with a half-saturation concentration of 50–100 mM, therefore, has to be attributed to a different process. Most likely it is a Na^+-induced shift in the $E_1P \leftrightarrow E_2P$ equilibrium via the extracellular Na^+ binding site.

Processes 2, 3, and 4 work in the same direction, namely to decrease the E_2P concentration in favor of E_1P. A lyotropic effect of Cl^- on the amplitudes of the capacitive signal (process 3) can be ruled out in the concentration range used here because an increase in Cl^- at constant Na^+ concentration did not affect the amplitudes (Fig. 6, *top*). An ionic strength effect can also be excluded on the basis of the same measurement. Processes 2 and 4 are difficult to discriminate: The extracellular Na^+ binding site has an affinity of ~600 mM (Taniguchi and Post, 1975), while Na^+ acting in the place of K^+ was reported at ~200 mM Na^+ (Nagel et al., 1987). In the following, we will only take into account the Na^+-induced shift of the $E_1P \leftrightarrow E_2P$ equilibrium. The influence of process 4 on the results will be discussed separately in the last section.

Na^+ dependence of the amplitudes

The amplitudes of the capacitive signal $\Delta I_y/\omega$ at low and high frequencies rise with a half-saturation value of ~100 mM (Fig. 5). The high half-saturation concentration demonstrates that this behavior is not determined by the formation of the phosphoenzyme. An appropriate kinetic model must, therefore, take into account the low-affinity extracellular Na^+ binding site as shown in Fig. 10. The two steps of the kinetic model are characterized by the relaxation times τ_{12} and τ_{Na} and by the equilibrium constants $K_{12} = [E_2PNa]/[(Na)E_1P]$ and $K_{Na}/[Na] = [E_2P]/[E_2PNa]$. Because the concentration of added Na^+ (c_{Na}) is much larger than the total enzyme concentration, we have pseudo-first-order Na^+ binding kinetics with $[Na] = c_{Na}$. The rate constants for the $E_1P \leftrightarrow E_2P$ transition are k^+ and k^-, with $\tau_{12}^{-1} = k^+ + k^-$ and $K_{12} = k^+/k^-$.

At low frequency ($\omega \ll \tau^{-1}$) the amplitude of the capacitive signal is proportional to the factor $c_A^0 \cdot c_B^0/(c_A^0 + c_B^0)$ (Eqs. 13 and 14). Equation 13 is strictly valid only for the simple one-step reaction (Eq. 1). However, on the basis of simple considerations, we can also calculate the amplitudes at the low and high frequency limits for the more complicated two-step model (Fig. 10) as shown below.

At the high frequency limit of the measurement, the applied frequency is in the range $(\tau_{12})^{-1} \ll \omega \ll (\tau_{Na})^{-1}$. Because $(\tau_{12})^{-1} \ll \omega$, the left-hand side of the kinetic model in Fig. 10, $(Na)E_1P \leftrightarrow E_2PNa$, is too slow to follow the applied potential. $(Na)E_1P$ remains constant, and only the electrogenic Na^+ binding equilibrium, $E_1PNa \leftrightarrow E_2P$, contributes to the capacitive signal. We can calculate this contribution by applying Eqs. 13 and A5 to this equilibrium and by using the relationships for K_{12} and K_{Na} given above. Because $\omega \ll (\tau_{Na})^{-1}$, Eq. 13 has to be used in its low frequency limit ($\omega \ll \tau^{-1}$) to yield the high frequency amplitude of the capacitive signal:

$$\Delta C_p = \frac{(C_m + C_p)^2}{C_m^2}\frac{e_0^2}{k_B T}\frac{[E_2PNa][E_2P]}{E_{tot}} = C_E \frac{c_{Na}K_{Na}K_{12}^2}{(K_{Na}K_{12} + c_{Na}(1 + K_{12}))^2} \quad (16)$$

with

$$C_E = \frac{(C_m + C_p)^2}{C_m^2}\frac{e_0^2}{k_B T}E_{tot}.$$

The parameter C_E is constant for a given experiment and depends only on temperature; the total protein concentration, $E_{tot} = [(Na)E_1P] + [E_2PNa] + [E_2P]$; and the electrical properties of the compound membrane.

In the low frequency limit, $\omega \ll (\tau_{Na})^{-1}$ and $\omega \ll (\tau_{12})^{-1}$, in addition to the Na^+ binding reaction, the $(Na)E_1P \leftrightarrow E_2PNa$ equilibrium can also follow the applied periodic perturbation and contributes (even if it is electroneutral itself) to the amplitude. We can account for this effect by taking $(Na)E_1P$ and E_2PNa together into a pool X_{12} with a modified rate constant $\tilde{k}_{Na}^+ = k_{Na}^+ K_{12}/(1 + K_{12})$. This is possible because $\omega \ll (\tau_{12})^{-1}$ and is analogous to the procedure used above for the derivation of the simplified model ($(Na)E_1P \leftrightarrow X_{Na}$). Then, the low frequency amplitude of the capacitive signal is given by

$$\Delta C_p = \frac{(C_m + C_p)^2}{C_m^2}\frac{e_0^2}{k_B T}\frac{([(Na)E_1P] + [E_2PNa])[E_2P]}{E_{tot}} = C_E \frac{c_{Na}K_{Na}K_{12}(1 + K_{12})}{(K_{Na}K_{12} + c_{Na}(1 + K_{12}))^2} \quad (17)$$

Equations 16 and 17 have been used as model functions for a simultaneous fit to the Na^+ dependence of the low and the high frequency amplitudes of the capacitive signal (Fig. 5). From the fit we obtained a Na^+ dissociation constant K_{Na} of 900 mM at the extracellular binding site and a constant K_{12} of 0.87. This means that (at pH 6.2) the rate constant for the reverse reaction of the $E_1P \leftrightarrow E_2P$ equilibrium is approximately equal to that of the forward reaction. This is a surprising finding because it shows that the conformational transition $E_1P \leftrightarrow E_2P$ is not displaced in the direction of transport by itself. It is rather the low extracellular affinity of E_2P for Na^+ (900 mM) that drives transport.

The capacitive signal at different pH

Both the frequency dependence and the amplitudes of the capacitive signal change with pH. This is not surprising, because rate constants and equilibrium binding constants are known to vary with pH. In Table 1 the parameters

determined in the electrical measurements at different pH values are summarized. A characteristic feature of the frequency spectrum is the ratio of the capacitive signals at low (10 Hz) and at high (1015 Hz) frequencies, $\Delta C_p^{1015}/\Delta C_p^{10}$. In terms of the kinetic model, ΔC_p^{1015} is described by Eq. 16, while ΔC_p^{10} is described by Eq. 17. From these equations a simple relationship can be derived relating $\Delta C_p^{1015}/\Delta C_p^{10}$ to the equilibrium constant K_{12}: $\Delta C_p^{1015}/\Delta C_p^{10} = K_{12}/(1 + K_{12})$. The values of K_{12} in Table 1 have been calculated using this expression. Also included in the table is the affinity of the extracellular Na^+ binding site, which has been determined from the Na^+ dependence of the capacitive signal (Fig. 5). This value is only available at pH 6.2. We can now combine the simplified model ($(Na)E_1P \leftrightarrow X_{Na}$), the relationship for the relaxation rate $\tau^{-1} = k^+ + \tilde{k}^-$, and $K_{12} = k^+/k^-$ to obtain k^+, $\tilde{k}^-$, and k^-, which are also included in the table. These values are given in bold face in Table 1.

The parameters in Table 1 show a marked variation with pH. The relaxation rate τ^{-1} is at maximum at physiological pH. Furthermore, the amplitude ratio $\Delta C_p^{1015}/\Delta C_p^{10}$ varies, yielding an equilibrium constant K_{12} that decreases with increasing pH. This means that the $E_1P \leftrightarrow E_2P$ transition is displaced more in the forward direction at acidic pH.

From the data shown in Fig. 5, absolute values for the amplitudes cannot be determined, because at each pH a separate experiment has to be performed that differs from the other by the amount of adsorbed protein. Therefore, pH titrations were made and the pH dependence of the amplitudes ΔC_p^{1015} and ΔC_p^{10} was measured (Fig. 8). Variation of the amplitudes of the capacitive signal can be brought about by a pH dependence of the kinetic parameters governing Na^+ transport. In terms of the kinetic model of Fig. 10, the amplitudes of the signal are described by Eqs. 16 and 17. Therefore, a pH dependence of the constants K_{12} or K_{Na} will result in pH-dependent amplitudes. K_{12} was determined separately and was found to change only moderately over the pH range 6.2–8.5 (Table 1). Using a constant value of K_{Na} of 900 mM, we calculated the pH dependence of ΔC_p^{1015} and ΔC_p^{10} and found that the variation in K_{12} could not account for the pH dependence of the amplitudes. Therefore, an additional variation of K_{Na} has to be considered. Setting $K_{Na} = 400$ mM at pH 7.4 and 200 mM at pH 8.5 yielded a pH dependence of the amplitudes (*dashed line* in Fig. 8) that was close to the observed values. Using these values for K_{Na}, we could also determine the rate constants of the conformational transition at pH 7.4 and 8.5 (see Table 1).

As shown above, the pH dependence of the amplitudes of the capacitive signal can be explained by a decrease in the equilibrium constant K_{12}, accompanied by a decrease in the dissociation constant K_{Na}. The latter accounts for the increase at acidic pH, while the former results in the decrease of the amplitudes in the basic pH range. Nevertheless, other possibilities for a pH dependence of the amplitudes have also to be considered; e.g., an amplitude variation could be brought about by a pH-dependent amount of phosphoenzyme. However, this can be ruled out because the rate of phosphoenzyme formation is much larger than the rate of its decay in the pH range 6.2–8.5 (Forbush and Klodos, 1991; Kane et al., 1997). Moreover, the transported charge may vary if acidic groups, which are believed to be part of cation binding sites, are protonated or deprotonated. However, this effect can only account for the decrease in the basic pH range.

For the analysis leading to the values in Table 1 an electroneutral conformational transition was assumed. Additional electrogenicity of the $E_1P \leftrightarrow E_2P$ transition would tend to raise the low frequency amplitude of the capacitive signal while leaving the high frequency amplitude unchanged. Under those conditions, equally good fits to the Na^+ dependence of the amplitudes could be obtained. However, the value of K_{12} obtained with our analysis would be too high. Therefore, the data in Fig. 5 do not rule out an electrogenic $E_1P \leftrightarrow E_2P$ transition. If this is considered a realistic possibility, then the real values for K_{12} would be somewhat lower than those given in Table 1. Additional effects of high Na^+ concentration (process 4; see above) have been neglected for the analysis. These would favor $(Na)E_1P$ and thereby yield an apparently higher Na^+ affinity at the extracellular binding site. The value for K_{Na} obtained from our analysis may, therefore, be too small and the real Na^+ dissociation constant may be slightly larger than that given in Table 1.

The rate constant of the $E_1P \leftrightarrow E_2P$ transition

We have shown above that the experimental results obtained in this study may be explained by a kinetic model consisting of an electroneutral $E_1P \leftrightarrow E_2P$ conformational transition followed by a electrogenic Na^+ binding/release reaction. How do the relaxation times determined for the rate-limiting conformational transition at pH 6.2–8.5 compare with values available in the literature? Using a periodic potential and lock-in detection, Lu et al. (1995) have reported a value of 880 s^{-1} at pH 7.0 and 38°C (200 s^{-1}) from giant patch-clamp experiments on guinea pig cardiac myocytes. Here and in the following the values in brackets have been calculated for 24°C, using an activation energy of 80 kJ/mol (Friedrich and Nagel, 1997), to allow a direct comparison with the values found here. Because the electrical relaxation method that we used is analogous to the voltage jump experiments (Sokolov et al., 1998), it is of interest to compare our results with relaxation rates obtained by this method. Using the whole-cell patch-clamp technique on cardiac myocytes, Nakao and Gadsby (1986) reported a relaxation rate of ~250 s^{-1} at pH 7.4 and 37°C (63 s^{-1}), while Rakowski (1993) found a value of ~180 s^{-1} at 22°C and pH 7.6 (225 s^{-1}), using *Xenopus* oocytes. From giant excised patch-clamp experiments on guinea pig cardiac myocytes, Hilgemann (1994) reported a biphasic behavior

of charge movement during a voltage step, with a rate constant of 400 s^{-1} at 37°C and pH 7.0 (100 s^{-1}) for the slower phase. Recently, Friedrich and Nagel (1997) determined a relaxation rate of 200 s^{-1} at 24°C and pH 7.4, using the same technique and preparation. From pig kidney membrane fragments (as used in our study), this rate constant was estimated to be $\geqslant$600 s^{-1} at 24°C and pH 7.4 by Kane et al. (1997). These results suggest a rate constant of 100–200 s^{-1} or even larger at 24°C for the $E_1P \leftrightarrow E_2P$ conformational transition. This agrees reasonably well with the relaxation times determined in this study of 192 s^{-1} (pH 6.2), 323 s^{-1} (pH 7.4), and 114 s^{-1} (pH 8.5) at 24°C. The strong pH dependence probably accounts for some of the variation found in the published values. Furthermore, intracellular regulation mechanisms may be effective, leading to differing results, as suggested from a comparison of whole cell (63 s^{-1}) and excised patch (200 s^{-1}) measurements on guinea pig cardiac myocytes (Nakao and Gadsby, 1986; Friedrich and Nagel, 1997).

Using the same technique as in our study, Sokolov et al. (1998) have investigated rabbit kidney Na^+/K^+-ATPase at room temperature and pH 6.5. Their experimental values as well as their interpretation are partially in disagreement with our study. Sokolov et al. (1998) determined a relaxation rate of ~1250 s^{-1}, which by comparison with a rate constant for the $E_1P \leftrightarrow E_2P$ transition, they assigned to the "release of the first Na^+ ion on the extracellular side of the Na^+/K^+-ATPase." For this comparison a value of the rate constant for the $E_1P \leftrightarrow E_2P$ transition of 200 s^{-1} at 37°C was chosen (Nakao and Gadsby, 1986), corresponding to 37 s^{-1} at 21°C (using an activation energy of 80 kJ/mol; Friedrich and Nagel, 1997). The values compiled above suggest, however, a much larger rate constant. As mentioned above, the value of Nakao and Gadsby (1986) may even be particularly low because of intracellular regulation. Indeed, for the Na^+/K^+-ATPase preparation used by Sokolov et al. (1998), a value of $\geqslant$260 s^{-1} at 24°C, pH 7.4 (Clarke et al., 1998) was reported and should be used for the comparison.

The relaxation rate determined in this study is much lower (192 s^{-1} at pH 6.2, 24°C) than the ~1250 s^{-1} reported by Sokolov et al. (1998). A possible explanation for the discrepancy found in the experimental values could be distortion of the data of Sokolov et al. (1998) by a high access resistance. As shown in Fig. 9 and as discussed at the beginning of the Discussion, a high access resistance $1/G_a$ tends to decrease the measured values at high frequencies, in which case the high frequency plateau may be missed and τ^{-1} shifts to higher frequencies. The speculation is supported by the fact that these authors find a much lower high-frequency plateau (0.13) than we do (0.45 at pH 6.2). This suggests that the relaxation time reported by Sokolov et al. (1998) is indeed too high, and a separate Na^+ release step with a rate constant of ~1250 s^{-1} is not required. Instead the rate constant obtained from the admittance measurement is most likely that of the rate-limiting $E_1P \leftrightarrow E_2P$ conformational transition.

Ionic strength and lyotropic anions

At high ionic strength, the relaxation time is drastically reduced. We determined $\tau^{-1} \leqslant 60$ s^{-1} at 130 mM NaCl + 500 mM choline chloride (data not shown), in agreement with Sokolov et al. (1998). This significant effect on the relaxation time cannot be explained by a lowering of the Na^+ affinity and a concomitant reduction of $\tilde{k}_-$, which can only account for a reduction of τ^{-1} from 192 s^{-1} to 166 s^{-1} (Table 1). At the same time, the relative free energy of the initial and the final state does not change (K_{12} = constant), as demonstrated by the constant ratio $\Delta C_p^{1015}/\Delta C_p^{10}$ (Fig. 6, *top*). The most straightforward explanation of this effect is an increase of the free energy of the transition state of the conformational transition at high ionic strength.

A different behavior is found for the lyotropic anion ClO_4^-. The equilibrium constant K_{12} calculated from $\Delta C_p^{1015}/\Delta C_p^{10}$ drops to zero at 400 mM ClO_4^-. Under these conditions, the enzyme is exclusively in the E_1P state. This direct effect of lyotropic anions on the conformational equilibrium is in agreement with a previous investigation of Suzuki and Post (1997).

Energetics of Na^+ transport

It is instructive to analyze the "basic free energy levels" (for a definition see Läuger, 1991) of the intermediates involved in the reaction. They can be calculated from the equilibrium constant K_{12} and the dissociation constant K_{Na} given in Table 1 according to the method of Läuger (1991): $\mu^0(E_2P) - \mu^0(E_2PNa) = -RT\ln(K_{Na}/c_{Na})$ and $\mu^0(E_2PNa) - \mu^0((Na)E_1P) = -RT\ln(K_{12})$. Here the "basic free energy level" of the intermediate E_i is $\mu^0(E_i)$, T is the absolute temperature, and R is the gas constant. The results for the three different pH values are shown in Fig. 10, where the free energy of the $(Na)E_1P$ state was arbitrarily set to zero.

It is clear from the figure that it is not the conformational transition that drives Na^+ transport. It is rather the formation of a very low-affinity Na^+ binding site accessible from the extracellular side that accounts for a forward-directed reaction in the cycle. This effect is most pronounced at acidic pH (see also K_{Na} in Table 1). Possibly a negatively charged acidic residue stabilizing Na^+ in the binding site becomes protonated under these conditions.

In the plasma membrane of the cell, Na^+ transport has to overcome the negative membrane potential. It is usually assumed that during Na^+ transport one positive charge is translocated across the membrane (Läuger, 1991). At a membrane potential of −60 mV this requires 5.8 kJ/mol. The overall exergonic reaction $(Na^+)E_1P$ to E_2P (−1.3 kJ/mol at physiological pH 7.4) can only compensate in part

for the energy requirement of Na^+ transport against a negative membrane potential, yielding an overall endergonic reaction (+4.5 kJ/mol). We could have anticipated for effective Na^+ translocation a "powerstroke," a "downhill" transition with a large amount of dissipated energy. This is not the case, as has been put forward by Stein (1990): "there is no need to postulate any particular power-stroke for the molecular engine." It is rather a sequence of small, approximately evenly distributed energy steps that makes an effective enzyme.

APPENDIX

Calculation of ΔG_p and ΔC_p from $\Delta \mathrm{Re}Y$ and $\Delta \mathrm{Im}Y$

The compound membrane consisting of the supporting bilayer and the adsorbed membrane fragments can be described by the equivalent circuit shown in Fig. 1 *B* (Bamberg et al., 1979). The planar lipid membrane is partially covered with membrane fragments containing Na^+/K^+-ATPase. The fraction not covered with membrane fragments is described by capacitance C_u, the covered fraction has the capacitance C_m, and the membrane fragments have a total capacitance of C_p. G_p is the leak conductance of the membrane fragments and G_a is the access conductance. The planar bilayer has a negligible conductance.

Neglecting G_a and ΔY_p, the complex total admittance of the equivalent circuit is given by

$$Y(\omega) = \frac{i\omega C_m(G_p + i\omega C_p)}{G_p + i\omega C_p + i\omega C_m} + i\omega C_u \tag{A1}$$

For sufficiently large frequencies ($\omega C_p \gg G_p$) the real part $\mathrm{Re}Y(\omega)$ and imaginary part $\mathrm{lm}Y(\omega)$ of the admittance are

$$\mathrm{Re}Y(\omega) = \frac{G_p C_m^2}{(C_p + C_m)^2}$$
$$\mathrm{Im}Y(\omega) = \omega\left(C_u + \frac{C_m C_p}{C_m + C_p}\right) \tag{A2}$$

The electrical activity of the Na^+/K^+-ATPase adds an additional component, the admittance Y_p. Because Y_p is in parallel with C_p and G_p, we can write the real part and the imaginary part of Y_p in terms of a conductivity and capacitance increment $\Delta Y_p = \Delta G_p + i\omega C_p$. In the following it is assumed that ΔC_p is small compared with C_p. (Because $\mathrm{Re}Y(\omega)$ depends on G_p in a linear fashion and $\mathrm{lm}Y(\omega)$ not at all, a similar constraint for ΔG_p is not required.) The increment in admittance, $\Delta Y(\omega) = \Delta \mathrm{Re}Y(\omega) + i\Delta \mathrm{lm}Y(\omega)$, upon a small increase in C_p and G_p can be calculated according to

$$\Delta \mathrm{Re}Y = \frac{\partial \mathrm{Re}Y}{\partial C_p}\Delta C_p + \frac{\partial \mathrm{Re}Y}{\partial G_p}\Delta G_p$$
$$\Delta \mathrm{Im}Y = \frac{\partial \mathrm{Im}Y}{\partial C_p}\Delta C_p + \frac{\partial \mathrm{Im}Y}{\partial G_p}\Delta G_p \tag{A3}$$

Solving these equations for ΔG_p and ΔC_p yields

$$\Delta G_p = -\frac{(C_m + C_p)^2}{C_m^2}\left(\frac{2G_p}{\omega(C_p + C_m)}\Delta \mathrm{Im}Y + \Delta \mathrm{Re}Y\right)$$
$$\Delta C_p = \frac{(C_m + C_p)^2}{C_m^2}\frac{\Delta \mathrm{Im}Y}{\omega} \tag{A4}$$

If $\Delta \mathrm{Re}Y$ and $\Delta \mathrm{lm}Y$ are of comparable magnitude, the first term in the equation for ΔG_p can be neglected because $\omega C_p \gg G_p$. Then the following equations hold:

$$\Delta G_p = -\frac{(C_m + C_p)^2}{C_m^2}\Delta \mathrm{Re}Y$$
$$\Delta C_p = \frac{(C_m + C_p)^2}{C_m^2}\frac{\Delta \mathrm{Im}Y}{\omega} \tag{A5}$$

An underlying assumption of the analysis leading to Eq. A5 is that the increment $\Delta C_p(\omega)$ is small compared with C_p. To estimate $\Delta C_p(\omega)$ we assume the membrane to be 1% covered with membrane fragments which corresponds to $\sim 10^{10}$ molecules/cm^2. This is consistent with current measurements (Fendler et al., 1993). Maximum $\Delta \mathrm{lm}Y_p$ and half-maximum $\Delta \mathrm{Re}Y_p$ are obtained at $c_A^0 = c_B^0 = c$ and at an angular frequency $\omega = \tau^{-1}$:

$$\Delta \mathrm{Re}Y_p = \Delta \mathrm{Im}Y_p = \frac{e_0^2}{4\tau k_B T}c \tag{A6}$$

With $\tau = 10$ ms, $T = 297$ K, and $c = 10^{10}$ cm^{-2}, we obtain $\Delta C_p = 1.5 \times 10^{-8}$ F cm^{-2}. This has to be compared with $C_p \approx 1 \times 10^{-6}$ F cm^{-2} and shows that the capacitance increments generated by the Na^+/K^+-ATPase are indeed considerably smaller than the capacitance of the membrane fragments.

The useful frequency range

Here the access resistance G_a has to be included. Before activation of the Na^+/K^+-ATPase by photolytic release of ATP, $\Delta Y_p(\omega) = 0$. Under these conditions the admittance of the equivalent circuit of Fig. 1 *B* is

$$Y(\omega) = \frac{\left(\dfrac{i\omega C_m(G_p + i\omega C_p)}{G_p + i\omega(C_p + C_m)} + i\omega C_u\right)\cdot G_a}{\dfrac{i\omega C_m(G_p + i\omega C_p)}{G_p + i\omega(C_p + C_m)} + i\omega C_u + G_a} \tag{A7}$$

After activation of the Na^+/K^+-ATPase, $\Delta Y_p(\omega) = \Delta G_p + i\omega\Delta C_p$. We can now substitute $G_p + \Delta G_p$ and $C_p + \Delta C_p$ for G_p and C_p in Eq. A7. The difference between the two results yields the increase in total admittance, $\Delta Y(\omega) = \Delta \mathrm{Re}Y + i\Delta \mathrm{lm}Y$, resulting from the activation of the Na^+/K^+-ATPase. From $\Delta \mathrm{Re}Y$ and $\Delta \mathrm{lm}Y$ one can calculate ΔG_p and ΔC_p and compare this with the original value. This calculation has been made for typical values of the equivalent circuit, using MATHCAD; it is shown in Fig. 9. We used $G_p = 1.5 \times 10^{-10}$ S, $C_p = 5 \times 10^{-11}$ F, $C_m = 2 \times 10^{-11}$ F, $C_u = 2 \times 10^{-9}$ F, and $G_a = 2.5 \times 10^{-5}$ S. This corresponds to a 1% coverage of the membrane with membrane fragments. For ΔG_p and $\omega\Delta C_p$ a value of 1.5×10^{-12} AV^{-1} was chosen.

We thank Eva Grabsch for excellent technical assistance, A. Schacht and E. Grell for the preparation of the Na^+/K^+-ATPase, and E. Bamberg for discussions and constant support. Special thanks to P. de Vries for helping with the preparation of the figures.

AB acknowledges with gratitude financial support from the Deutscher Akademischer Austauschdienst, the Max Planck Gesellschaft, and the TEMPUS project S-JEP-07393/95.

REFERENCES

Apell, H.-J., R. Borlinghaus, and P. Läuger. 1987. Fast charge translocations associated with partial reactions of the Na,K-pump. II. Microscopic analysis of transient currents. *J. Membr. Biol.* 97:179–191.

Bamberg, E., H.-J. Apell, N. A. Dencher, W. Sperling, H. Stieve, and P. Läuger. 1979. Photocurrents generated by bacteriorhodopsin on planar bilayer membranes. *Biophys. Struct. Mech.* 5:277–292.

Benz, R., and K. Janko. 1976. Voltage-induced capacitance relaxation of lipid bilayer membranes. Effects of membrane composition. *Biochim. Biophys. Acta.* 455:721–738.

Bernasconi, C. F. 1976. Relaxation Kinetics. Academic Press, New York.

Borlinghaus, R., H.-J. Apell, and P. Läuger. 1987. Fast charge translocations associated with partial reactions of the Na,K-pump. I. Current and voltage transients after photochemical release of ATP. *J. Membr. Biol.* 97:161–178.

Clarke, R. J., D. J. Kane, H.-J. Apell, M. Roudna, and E. Bamberg. 1998. Kinetics of Na^+-dependent conformational changes of rabbit kidney Na^+,K^+-ATPase. *Biophys. J.* 75:1340–1353.

De Weer, P., D. C. Gadsby, and R. F. Rakowski. 1988. Voltage dependence of the Na-K pump. *Annu. Rev. Physiol.* 50:225–241.

Fendler, K., E. Grell, and E. Bamberg. 1987. Kinetics of pump currents generated by the Na^+,K^+-ATPase. *FEBS Lett.* 1:83–88.

Fendler, K., E. Grell, M. Haubs, and E. Bamberg. 1985. Pump currents generated by the purified Na^+/K^+-ATPase from kidney on black lipid membranes. *EMBO J.* 4:3079–3085.

Fendler, K., S. Jaruschewski, A. Hobbs, W. Albers, and J. P. Froehlich. 1993. Pre-steady-state charge translocation in NaK-ATPase from eel electric organ. *J. Gen. Physiol.* 102:631–666.

Forbush, B., III, and I. Klodos. 1991. Rate limiting steps in Na^+ translocation by the Na/K pump. *Soc. Gen. Physiol. Ser.* 46:210–225.

Friedrich, T., E. Bamberg, and G. Nagel. 1996. Na^+,K^+-ATPase pump currents in giant excised patches activated by an ATP concentration jump. *Biophys. J.* 71:2486–2500.

Friedrich, T., and G. Nagel. 1997. Comparison of Na^+,K^+-ATPase pump currents activated by ATP concentration or voltage jumps. *Biophys. J.* 73:186–194.

Gadsby, D. C., M. Nakao, A. Bahinski, G. Nagel, and M. Suenson. 1992. Charge movements via the Na,K-ATPase. *Acta Physiol. Scand.* 146: 111–123.

Gadsby, D. C., R. F. Rakowski, and P. De Weer. 1993. Extracellular access to the Na,K pump: pathway similar to ion channel. *Science.* 260: 100–103.

Ganea, C., A. Babes, C. Lüpfert, E. Grell, K. Fendler, and R. J. Clarke. 1999. Effects of lyotropic anions on the kinetics of partial reactions of the Na^+,K^+-ATPase. *Biophys. J.* 77:267–281.

Glynn, I. M. 1985. The Na^+,K^+-transporting adenosine triphosphatase. *In* The Enzymes of Biological Membranes. A. N. Martonosi, editor. Plenum Press, New York. 35–113.

Glynn, I. M. 1993. All hands to the sodium pump. *J. Physiol. (Lond.).* 462:1–30.

Heyse, S., I. Wuddel, H.-J. Apell, and W. Stürmer. 1994. Partial reactions of the Na,K-ATPase: determination of rate constants. *J. Gen. Physiol.* 104:197–240.

Hilgemann, D. W. 1994. Channel-like function of the Na,K pump probed at microsecond resolution in giant membrane patches. *Science.* 263: 1492–1432.

Hobbs, A. S., R. W. Albers, and J. P. Froehlich. 1988. Complex time dependence of phosphoenzyme formation and decomposition in electroplax Na,K-ATPase. *Prog. Clin. Biol. Res.* 268A:307–314.

Jørgensen, P. L. 1974. Purification and characterization of $(Na^+ + K^+)$-ATPase. III. Purification from the outer medulla of mammalian kidney after selective removal of membrane components by sodium dodecylsulphate. *Biochim. Biophys. Acta.* 356:36–52.

Kane, D. J., K. Fendler, E. Grell, E. Bamberg, K. Taniguchi, J. P. Froehlich, and R. J. Clarke. 1997. Stopped-flow kinetic investigations of conformational changes of pig-kidney Na^+,K^+-ATPase. *Biochemistry.* 17:13406–13420.

Läuger, P. 1991. Electrogenic Ion Pumps. Sinauer Associates, Sunderland, MA.

Lu, C.-C., A. Kabakov, V. S. Markin, S. Mager, G. A. Frazier, and D. W. Hilgemann. 1995. Membrane transport mechanisms probed by capacitance measurements with megahertz voltage-clamp. *Proc. Natl. Acad. Sci. USA.* 92:11220–11224.

McCray, J. A., L. Herbette, T. Kihara, and D. R. Trentham. 1980. A new approach to time-resolved studies on ATP-requiring biological systems: laser flash photolysis of caged ATP. *Proc. Natl. Acad. Sci. USA.* 77: 7237–7241.

Nagel, G., K. Fendler, E. Grell, and E. Bamberg. 1987. Na^+ currents generated by the purified $(Na^+ + K^+)$-ATPase on planar lipid membranes. *Biochim. Biophys. Acta.* 901:239–249.

Nakao, M., and D. C. Gadsby. 1986. Voltage-dependence of Na^+ translocation by the Na/K-pump. *Nature.* 323:628–630.

Rakowski, R. F. 1993. Charge movement by the Na/K pump in *Xenopus* oocytes. *J. Gen. Physiol.* 101:117–144.

Rakowski, R. F., D. C. Gadsby, and P. de Weer. 1997. Voltage dependence of the Na/K-pump. *J. Membr. Biol.* 155:105–112.

Scales, D., and G. Inesi. 1976. Assembly of ATPase protein in sarcoplasmic reticulum membrane. *Biophys. J.* 16:735–751.

Sokolov, V. S., K. V. Pavlov, and K. N. Dzhandzhugazyan. 1994. Change of membrane capacitance coupled with electrogenic transport by Na,K-ATPase. *In* The Sodium Pump: Structure, Mechanism, Hormonal Control and Disease. W. Schöner and E. Bamberg, editors. Steinkopff, Darmstadt. 529–533.

Sokolov, V. S., S. M. Stukolov, A. S. Darmostuk, and H.-J. Apell. 1998. Influence of sodium concentration on changes of membrane capacitance associated with the electrogenic ion transport by the Na,K-ATPase. *Eur. Biophys. J.* 27:605–617.

Stein, W. D. 1990. Energetics and the design principles of the Na/K-ATPase. *J. Theor. Biol.* 147:145–159.

Stürmer, W., R. Bühler, H.-J. Apell, and P. Läuger. 1991. Charge translocation by the Na,K-pump. II. Ion binding and release at the extracellular face. *J. Membr. Biol.* 121:163–176.

Suzuki, K., and R. L. Post. 1997. Equilibrium of phosphointermediates of sodium and potassium ion transport adenosine triphosphatase: action of sodium ion and Hofmeister effect. *J. Gen. Physiol.* 109:537–554.

Taniguchi, K., and R. L. Post. 1975. Synthesis of adenosine triphosphate and exchange between inorganic phosphate and adenosine triphosphate in sodium and potassium ion transport adenosine triphosphatase. *J. Biol. Chem.* 250:3010–3018.

Walker, J. W., G. P. Reid, J. A. McCray, and D. R. Trentham. 1988. Photolabile 1-(2-nitrophenyl) ethyl phosphate esthers of adenine nucleotide analogues. Synthesis and mechanism of photolysis. *J. Am. Chem. Soc.* 110:7170–7177.

Wuddel, I., and H.-J. Apell. 1995. Electrogenicity of the sodium transport pathway in the Na,K-ATPase probed by charge-pulse experiments. *Biophys. J.* 69:909–921.